



Dual Src and Abl inhibitors target wild type Abl and the AblT315I Imatinib-resistant mutant with different mechanisms

Emmanuele Crespan^a, Marco Radi^b, Samantha Zanoli^a, Silvia Schenone^c, Maurizio Botta^{b,*}, Giovanni Maga^{a,*}

^a Institute of Molecular Genetics IGM-CNR, via Abbiategrasso 207, 27100 Pavia, Italy

^b Dept. of Chemistry and Pharmaceutical Technology, University of Siena, via Banchi di Sotto 55, 53100 Siena, Italy

^c Dept. of Pharmaceutical Sciences, University of Genova, Viale Benedetto XV 3, 16132 Genova, Italy

ARTICLE INFO

Article history:

Received 18 February 2010

Revised 6 April 2010

Accepted 7 April 2010

Available online 18 April 2010

Keywords:

Src
Abl
Anticancer chemotherapy
Drug resistance
Enzyme kinetics
Tyrosine kinases

ABSTRACT

The tyrosine kinase Src and its close homolog Abl, both play important roles in chronic myelogenous leukemia (CML) progression and Imatinib resistance. No clinically approved inhibitors of the drug-resistant AblT315I exist to date. Here, we present a thorough kinetic analysis of two potent dual Src-Abl inhibitors towards wild type Src and Abl, and the AblT315I mutant. Our results show that the most potent compound BO1 shows only a modest loss of potency (fourfold) towards the AblT315I mutant in vitro and was an ATP-competitive inhibitor of wild type Abl but it acted as a non-competitive inhibitor in the case of AblT315I.

© 2010 Elsevier Ltd. All rights reserved.

1. Introduction

Despite the past efforts to develop selective targeted therapies for the treatment of cancer, the aim has recently turned to find compounds acting on multiple targets in order to face the drug resistance often connected to the activation of alternative signaling pathways.¹ Multiple-kinase inhibitors currently approved for cancer chemotherapy include Lapatinib (which targets HER1 and HER2 receptorial kinases) as well as Sorafenib, targeting VEGFR, RAF and PDGFR kinases. Imatinib itself has been shown to act not only on Bcr-Abl, but also on KIT and PDGFR kinases.^{2,3} Targeting the chronic myelogenous leukemia (CML)-specific Bcr-Abl tyrosine kinase has proved to be a successful therapeutic approach. In fact, the non-receptor tyrosine kinase c-Abl, the cellular counterpart of Bcr-Abl, even though is normally implicated in various cellular processes, is not an essential enzyme.⁴ Recent results established a functional link between Bcr-Abl and the Src family tyrosine kinases (SFKs), that play an important role in the cellular adhesion and motility as well as in the growth, progression, and metastasis of a variety of human malignancies such as colon,

breast, pancreas, lung, and brain cancers. Studies with Src dominant negative mutants suggested that Src kinases play a role in proliferation of Bcr-Abl expressing cell lines¹ and overexpression of Src kinases is implicated in Bcr-Abl-mediated leukemogenesis and in Imatinib resistance. Abl shares significant sequence homology and remarkable structural resemblance in its active state with Src family members. For this reason, several ATP-competitive inhibitors targeting the active conformation of the enzyme (differently from Imatinib that binds the catalytically inactive form) originally developed as Src inhibitors, showed to be also potent Abl inhibitors. For example, Dasatinib (Sprycel™), by Bristol Myers Squibb, is the first dual Src-Abl inhibitor approved by FDA (June 28, 2006) for the treatment of CML patients with resistance or intolerance to prior therapy, including Imatinib.⁵

Although these second-generation 'dual' tyrosine kinase inhibitors have shown to be clinically effective against most of the Imatinib-resistant mutants,⁶ to date poor results have been obtained in the treatment of the Bcr-Abl T315I mutant and no clinically approved T315I inhibitors are still on the market.⁷ Alternative approaches for the inhibition of the T315I mutant are of great pharmacological interest and novel inhibitors are still needed.

By a combination of molecular modeling and combinatorial chemistry techniques, our research group has recently synthesized two different class of inhibitors: pyrazolo[3,4-d]pyrimidines (generic structure **1**, Fig. 1) and the 1,3,4-thiadiazole derivatives

* Corresponding authors. Tel.: +39 0382546354; fax: +39 0382422286 (G.M.); tel.: +39 0577234306; fax: +39 0577232188 (M.B.).

E-mail addresses: botta.maurizio@gmail.com (M. Botta), maga@igm.cnr.it (G. Maga).

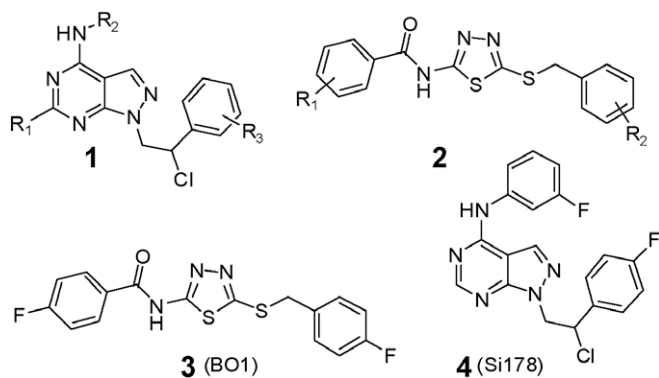


Figure 1. Generic structure of pyrazolo[3,4-*d*]pyrimidine inhibitors (**1**), of 1,3,4-thiadiazole derivatives (**2**) and of the compounds studied in this work (**3** and **4**).

(generic structure **2**, Fig. 1). The pyrazolo[3,4-*d*]pyrimidines are Src inhibitors endowed with potent antiproliferative and proapoptotic activity toward A431 (epidermoid) and 8701-BC (breast cancer) cell lines overexpressing Src.^{8,9} In addition, these compounds were able to inhibit proliferation of three Bcr-Abl-positive human leukemia cell lines (K-562, KU-812, and MEG-01), to reduce Bcr-Abl tyrosine phosphorylation and to promote apoptosis of Bcr-Abl-expressing cells through directly inhibition of Abl activity.¹⁰ A model for the T3151 mutant was used to identify, within our collection of pyrazolo[3,4-*d*]pyrimidines, potential inhibitors of the mutated enzyme. The selected compounds resulted active against wt Bcr-Abl (Imatinib-sensitive) or three of the most common Imatinib-resistant mutants T3151, Y253F, and E255 K.¹¹

The 1,3,4-thiadiazole derivatives were identified applying a computational protocol, based on docking/molecular dynamics simulations and on a pharmacophore-based database search. This study led to the identification of a few hit compounds that were later optimized to give compound BO1 (**3**) which showed high potency of inhibition in enzymatic assays and a promising biological profile on Imatinib-sensitive and Bcr-Abl-independent Imatinib-resistant leukemia cells, being able to reduce the clonogenic activity ($LD_{50} = 2.2 \mu\text{M}$) of Bcr-Ab l-expressing clones.^{12–14} Docking studies demonstrated that compounds **1** and **2** are ATP-competitive inhibitors and bind to the active conformation of the enzyme.^{13,15}

As a first step towards a better understanding of the molecular determinants for the dual-inhibitory activity of these two classes of compounds against Src and Abl, we have performed a thorough kinetic analysis on the two representative dual Src-Abl inhibitors BO1 (**3**) and SI178 (**4**). The mechanism of inhibition of these two compounds towards wild type Src and Abl and the T3151 Abl mutant has been studied. Our results show that these molecules have the same mechanism of action on wt Src and Abl. Interestingly, the most potent derivative BO1 (**3**) is significantly active towards the T3151 mutated Abl, but with a different mechanism with respect to Abl wild type. These data will be useful for the development of novel, more potent dual Src-Abl inhibitors.

2. Results

2.1. Kinetic analysis of the reactions catalyzed by Src and Abl

The tyrosine kinases Src and Abl need to bind two substrates (ATP and the peptide) before the products (ADP and phosphotyrosine peptide) can be released. The general reaction pathway for an enzyme acting on two substrates is schematically drawn in Figure 2. The microscopic rates of each step are indicated as well as their relationships with the four equilibrium constants K_s^{ATP} , K_m^{ATP} , K_s^{pep}

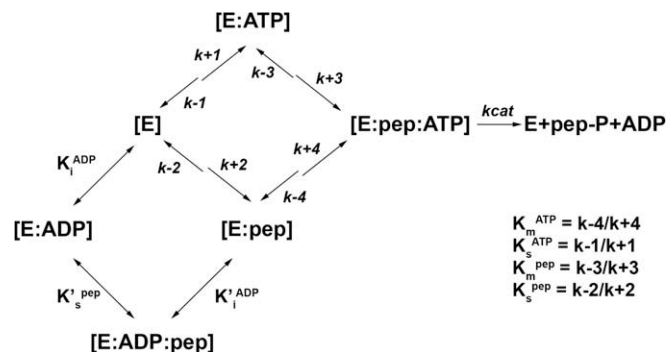


Figure 2. General reaction pathway for a two substrates–two products [bi–bi] sequential reaction. Product [ADP] inhibition pathway is also indicated in the bottom left part. For details see Section 5.

and K_m^{pep} . The kinetic mechanism for this pathway is represented by Eq. (1) (see Section 5). This general kinetic model is valid without any assumption on the relative order of binding of the reactants to the enzyme. In order to precisely determine the reaction pathway, we derived the four kinetic constants (K_s^{ATP} , K_m^{ATP} , K_s^{pep} and K_m^{pep}) for both substrates of the reaction. The variation of the reaction velocity was measured at fixed concentrations of one substrate, as a function of increasing concentrations of the other, and analyzed according to the Michaelis–Menten equation. Figure 3A and B shows the curves obtained for Src by varying the peptide and ATP substrates, respectively. Figure 3C and D shows the same experiments in the presence of Abl. The apparent maximal reaction rates (V_{maxapp}) obtained for each substrate were then plotted as a function of the corresponding substrate concentrations to obtain the K_m^{ATP} and K_m^{pep} values for Src and Abl (Fig. 4A and B). To obtain the K_s values for each substrate, the variation of the apparent K_m values (K_{mapp}) values obtained from the plots shown in Figure 3A–D was studied as a function of the varying substrates. As shown in Figure 4C and D, in the case of Src, the K_{mapp} for either substrate was decreased by increasing concentrations of the other substrate. Fitting of the curves to (Eqs. (2) and (3)) (see Section 5) allowed the determination of the K_s^{pep} and K_s^{ATP} values. In the case of Abl, an opposite behavior was observed, so that the K_{mapp} values for one substrate were increased by increasing concentrations of the other substrate (Fig. 4E and F). The data were fitted to a linear relationship (Eqs. (4) and (5) in Section 5) and the corresponding K_s^{pep} and K_s^{ATP} were derived. The opposite trend of K_{mapp} values variation observed for Src and Abl did not reflect any particular mechanism, since it depended only on the particular combinations of the microscopic rates contained in the K_m and K_s values (Fig. 2).

2.2. Src and Abl tyrosine kinases follow a random bi–bi reaction mechanism

Having determined all four equilibrium constants for the binding of the two substrates to each enzymatic form along the reaction pathway (Fig. 2), their values can be compared to sort out the reaction mechanism. The calculated values are reported in Table 1. As can be seen, both substrates show comparable dissociation constants from the free enzyme (K_s values), as well as from the enzyme–substrate complex (K_m values). A difference exists, however, between K_m and K_s values, with the latter generally lower than the former. Thus, it does not seem that either Src or Abl bind their substrates in any particular order, since both ATP and the peptide have equal chances of combining with either the free enzyme or the enzyme–substrate complex. The general kinetic model shown in Eq. (1) predicts that, in the case of a random order of substrate addition, a relationship exists between the four equilibrium constants (Eq. (6)), so that any of them could be calculated

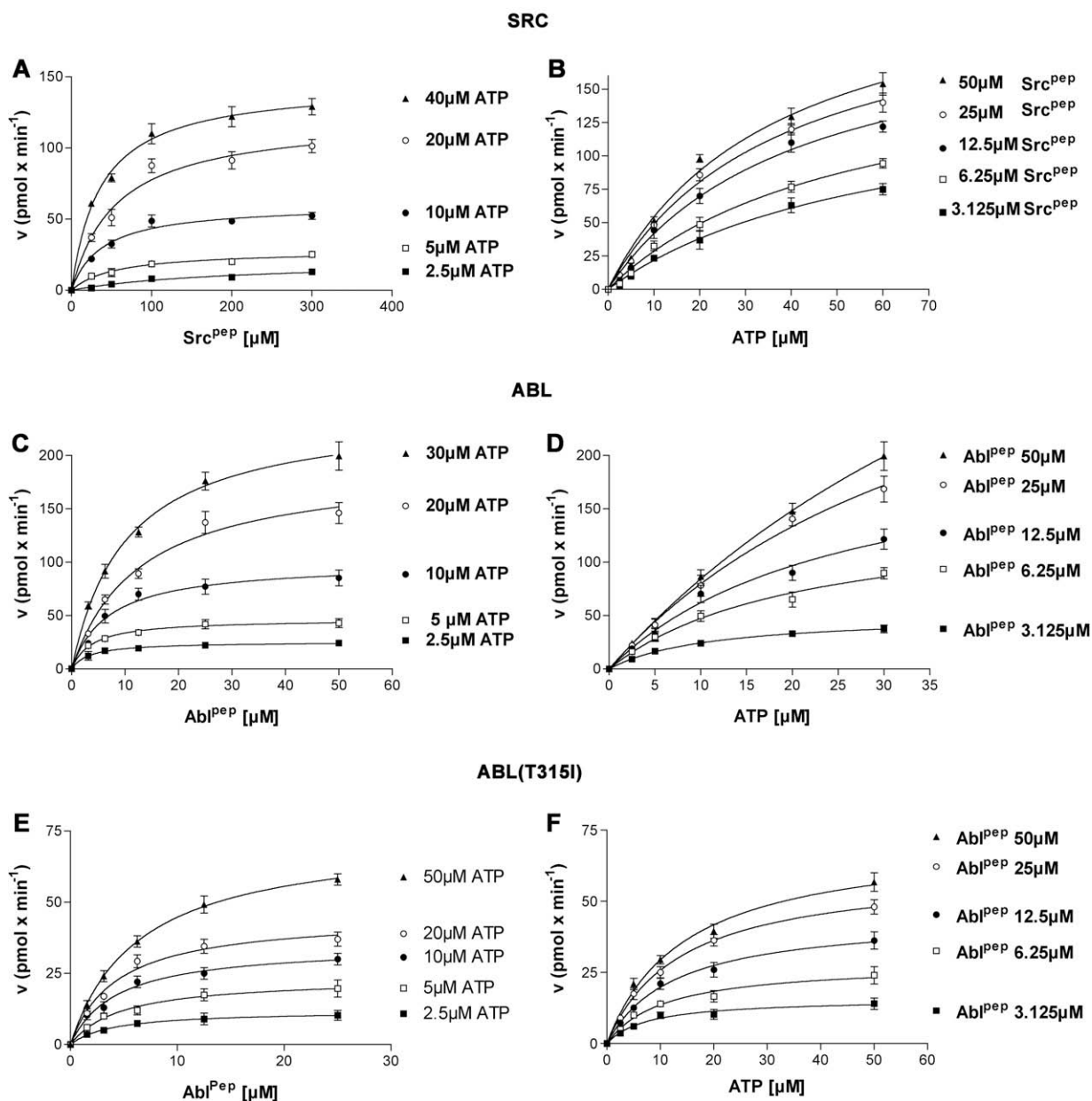


Figure 3. Kinetic analysis of kinase reactions of Abl and Src. Each reaction was performed as described in Section 5. Values are the means of three independent experiments. Error bars represent \pm S.D. (A) Variation of the reaction velocity of Src as function of Src peptide substrate concentration at different fixed concentrations of ATP. (B) Variation of the reaction velocity of Src as function of ATP concentration at different fixed concentrations of Src peptide substrate. (C) Variation of the reaction velocity of Abl as function of Abl peptide substrate concentration at different fixed concentrations of ATP. (D) Variation of the reaction velocity of Abl as function of ATP concentration at different fixed concentrations of Abl peptide substrate. (E) Variation of the reaction velocity of AblT315I as function of Abl peptide substrate concentration at different fixed concentrations of ATP. (F) Variation of the reaction velocity of AblT315I as function of ATP concentration at different fixed concentrations of Abl peptide substrate.

Table 1
Equilibrium binding and steady-state kinetic constants for the interaction of Src and Abl with their substrates

K_m^{ATP} , μ M	K_s^{ATP} , μ M	K_m^{pep} , μ M	K_s^{pep} , μ M
<i>Src</i> ^a			
30 \pm 5	14 \pm 1	23 \pm 3	13 \pm 1
<i>Abl</i> ^a			
33 \pm 5	12 \pm 2	20 \pm 2	13 \pm 3
<i>Abl T315I</i> ^a			
6 \pm 2	16 \pm 5	5 \pm 1	25 \pm 3

^a Values are the means of three independent experiments \pm S.D.

from the other three. To verify whether such a relationship holds for the values obtained, we calculated each of the four constants through Eq. (6) and compared the theoretical values with the ones experimentally determined. The calculated values for K_s^{ATP} , K_m^{ATP} , K_s^{pep} and K_m^{pep} were 17 μ M, 25 μ M, 11 μ M, and 28 μ M, respectively, for Src, and 21 μ M, 19 μ M, 25 μ M, and 18 μ M, respectively, for Abl. These values are in good agreement (less than 1.5-fold difference) with the experimentally derived ones shown in Table 1, further supporting a random order of substrate addition for both enzymes.

2.3. Product inhibition studies of Src and Abl reactions

According to the mechanism depicted in Figure 2, ADP, one of the products of the reaction, should be able to compete only with

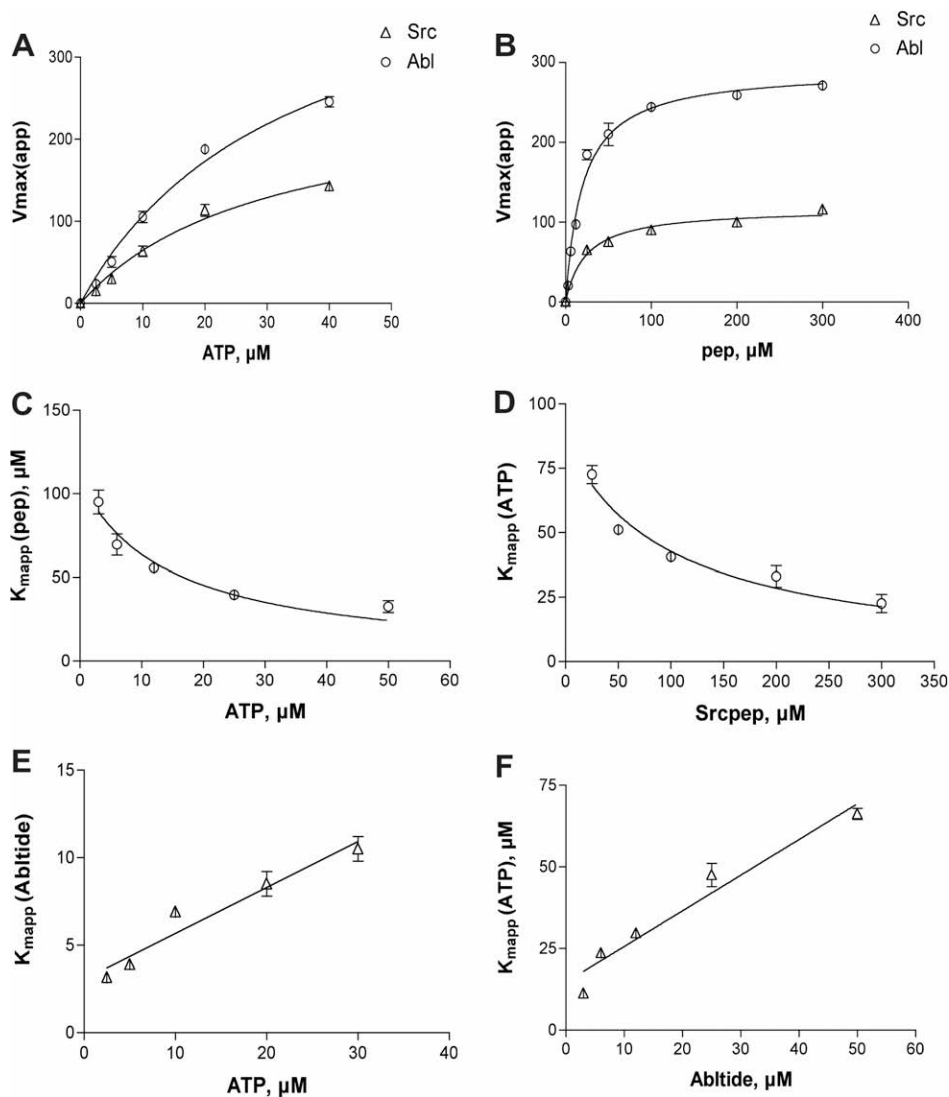


Figure 4. Determination of the reaction mechanism of Src and Abl. Data analysis was performed as described in the Section 5. Values are the means of three independent experiments. Error bars represent \pm S.D. (A) Variation of the $V_{\max\text{app}}$ values for Src (triangles) and Abl (circles) reactions, determined as shown in Figure 3, as a function of ATP concentrations. (B) Variation of the $V_{\max\text{app}}$ values for Src [triangles] and Abl [circles], determined as shown in Figure 3, as a function of the peptide substrate concentrations. (C) Variation of the K_{mapp} values of Src for the peptide substrate determined as shown in Figure 3, as a function of the ATP substrate concentration. (D) Variation of the K_{mapp} values of Src for the ATP substrate, determined as shown in Figure 3, as a function of the peptide substrate concentration. (E) Variation of the K_{mapp} values of Abl for the peptide substrate determined as shown in Figure 3, as a function of the ATP substrate concentration. (F) Variation of the K_{mapp} values of Abl for the ATP substrate, determined as shown in Figure 3, as a function of the peptide substrate concentration.

its parent substrate (i.e., ATP). In order to verify this, inhibition experiments were carried out by titrating increasing amounts of ADP in the presence of a fixed subsaturating concentration of one substrate and varying the concentration of the other substrate. The resulting mechanism of inhibition with respect to each sub-

strate of the reaction is reported in Table 2, along with the corresponding apparent ADP dissociation constant (K_i). As can be seen, ADP was a competitive inhibitor with respect to ATP. These results indicated that, as expected for a random order equilibrium reaction, the product ADP affects only the binding of the parent substrate, increasing the K_s^{ATP} and K_m^{ATP} values, without affecting the binding of the peptide. Since the K_s^{ATP} value is different from K_m^{ATP} (Table 1), a mixed-type mechanism, rather than a purely non-competitive one, was observed when ADP was tested by varying the peptide substrate (Table 2).

2.4. The T315I mutation of Abl alters the binding of the substrates to the enzyme

Next, we analyzed the reaction mechanism of the Imatinib-resistant Abl mutant T315I. Figure 3E and F shows the primary plots obtained by varying one substrate in the presence of fixed amount of the other. From these data, the four kinetic constants

Table 2
Product inhibition of Src and Abl with respect to ADP

K_i^{ADP} , μM	Variable substrate	Type of inhibition
Src ^a		
45 \pm 5	ATP	Competitive
56 \pm 6	Peptide	Mixed non-competitive
Abl ^a		
56 \pm 5	ATP	Competitive
100 \pm 10	Peptide	Mixed

^a Values are the means of three independent experiments \pm S.D.

K_s^{ATP} , K_m^{ATP} , K_s^{pep} and K_m^{pep} were derived as described above. The calculated values are reported in Table 1. Again, they indicate a random order mechanism of substrate binding. However, contrary to Abl wt, the K_m^{ATP} and K_m^{pep} values of the T315I mutant were lower than the corresponding K_s values, indicating that either substrate showed higher affinity for the enzyme bound to the other substrate than for the free enzyme. In addition, the Michaelis constant for ATP binding showed absolute values lower than the corresponding ones for the Abl wt enzyme, suggesting that the T315I mutant had higher affinity for the ATP substrate. The T315I mutation partially occludes an hydrophobic pocket located at the rear of the ATP

binding site. In addition, it apparently stabilizes the activation loop of the enzyme into an 'active-like' conformation. Thus, it is possible that these structural changes alter the conformation of the enzyme–substrate complexes with respect to the wild type enzyme.

2.5. Kinetic analysis of the inhibition of wt Src and Abl by compounds BO1 (3) and SI178 (4)

The kinetic analysis presented above allowed us to determine a minimal reaction pathway for the tyrosine kinases Src, Abl and

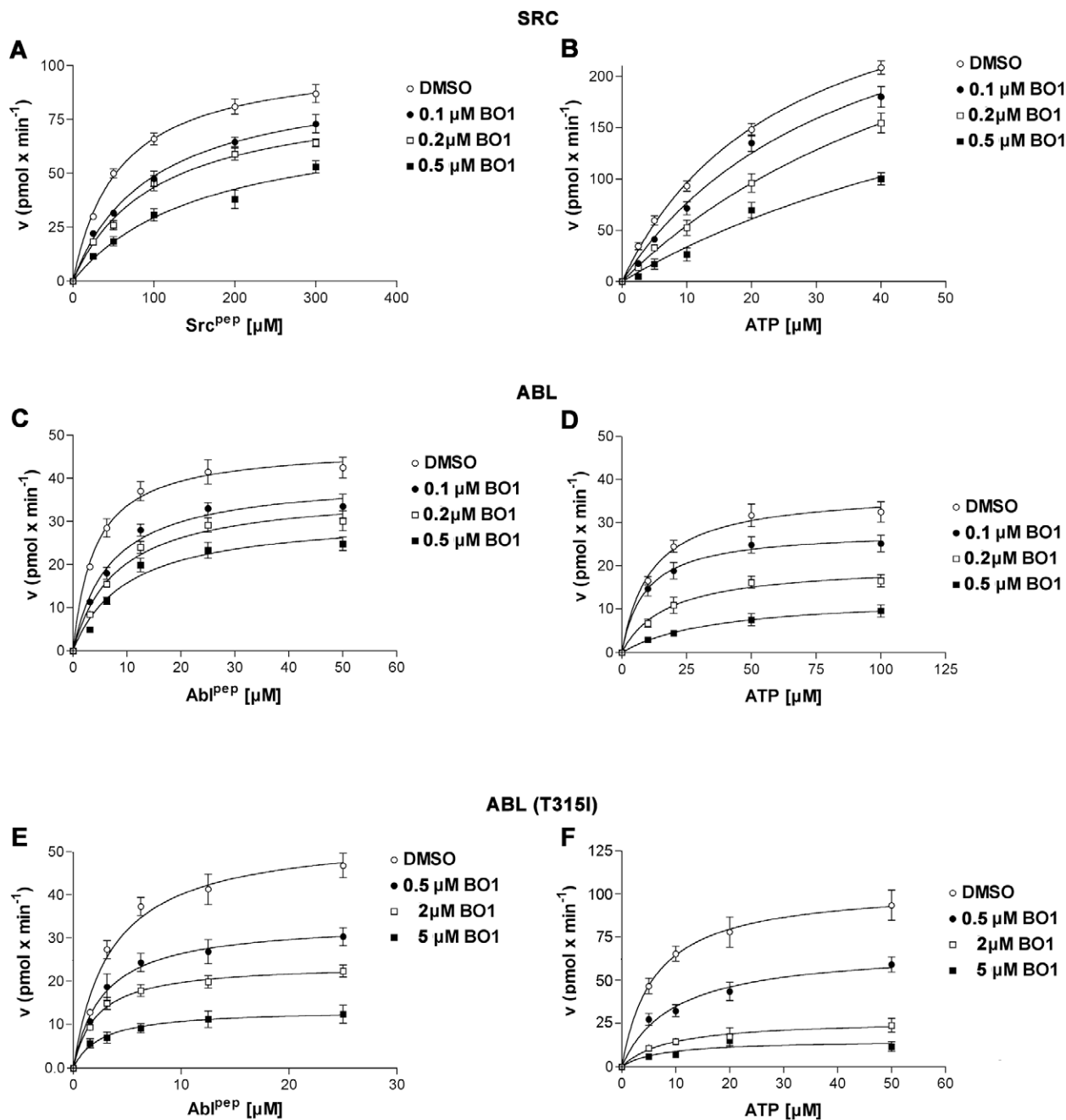


Figure 5. Kinetic analysis of kinase reactions of Src, Abl and AblT315I in the presence of different concentration of BO1. Each reaction was performed as described in Section 5. Values are the means of three independent experiments. Error bars represent \pm S.D. (A) Variation of the reaction velocity of Src as function of Src peptide substrate concentration at different fixed concentrations of BO1. (B) Variation of the reaction velocity of Src as function of ATP concentration at different fixed concentrations of BO1. (C) Variation of the reaction velocity of Abl as function of Abl peptide substrate concentration at different fixed concentrations of BO1. (D) Variation of the reaction velocity of Abl as function of ATP concentration at different fixed concentrations of BO1. (E) Variation of the reaction velocity of AblT315I as function of Abl peptide substrate concentration at different fixed concentrations of BO1. (F) Variation of the reaction velocity of AblT315I as function of ATP concentration at different fixed concentrations of BO1.

AblT315I. These informations were essential for the following investigation of the mechanism of inhibition of two selected compounds BO1 (3) and SI178 (4) which represent the progenitor of the two classes of inhibitors developed by our group.

We analyzed the reaction velocity as a function of each substrate of the reaction, holding the other at a fixed subsaturating amount and in the presence of increasing amounts of the inhibitor to be tested. As an example, Figure 5 shows the primary plots obtained for the compound BO1 with Src (panels A, B) and Abl (panels C, D).

The variations of the apparent V_{max} and K_m values for each substrate were studied as a function of the inhibitor concentration. As

an example, Figure 6 shows the results of this analysis for the compound BO1. As can be seen, in the case of Src (Fig. 6A and B) the K_{mapp} values for the ATP and the peptide substrate were increased by the inhibitor, whereas the V_{maxapp} values were not affected. In the case of Abl, an increase in the K_{mapp}^{ATP} was observed with no effects on the V_{maxapp} (Fig. 6C), whereas the inhibitor affected both the K_{mapp}^{pep} (increased) and the V_{maxapp} (decreased) values (Fig. 6D). The same behavior was observed for the inhibitor SI178 (data not shown). The calculated K_i values as well as the corresponding inhibitory mechanisms are listed in Table 3. The compound SI178 resulted sevenfold more active towards Src than Abl. Conversely, BO1 inhibited Abl fivefold more than Src.

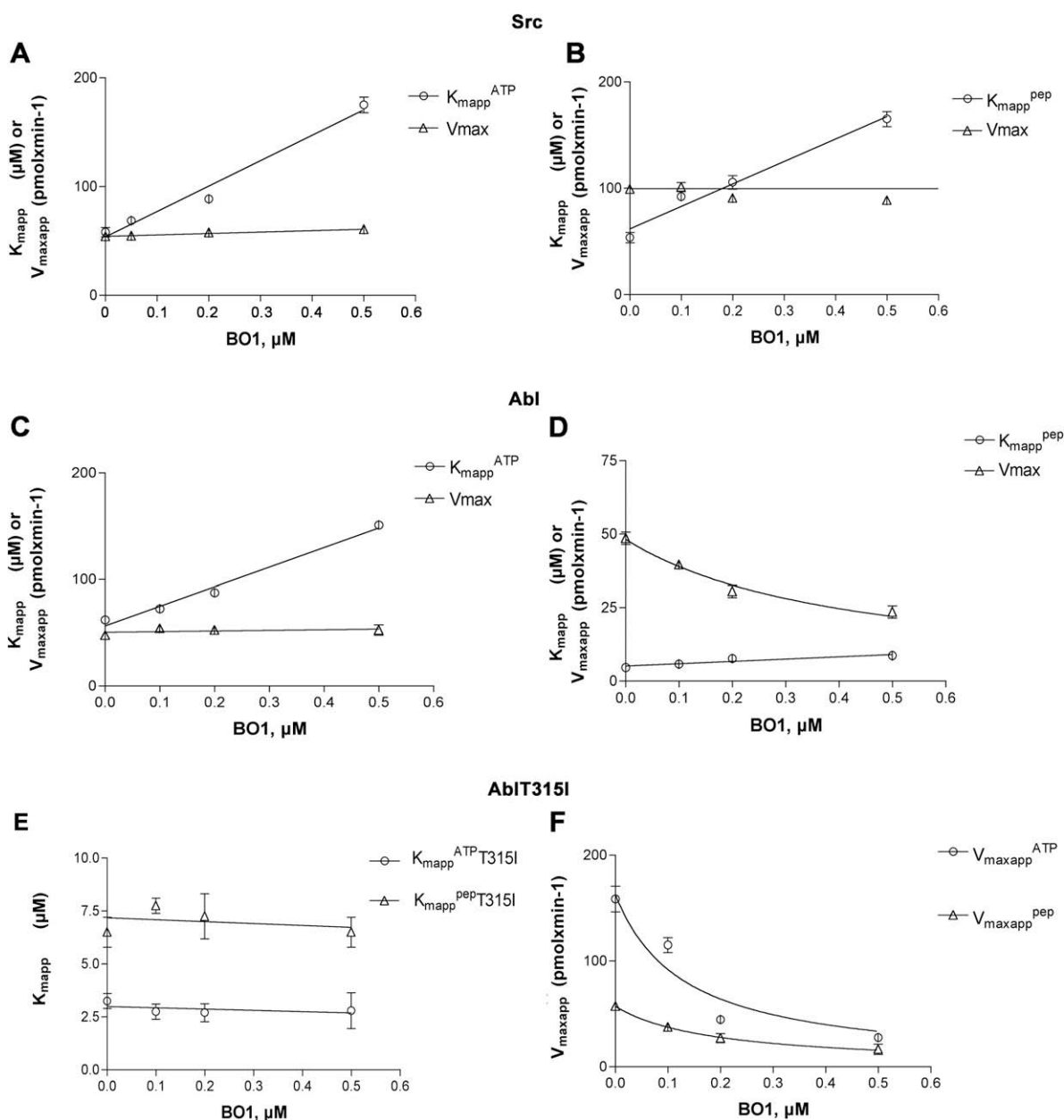


Figure 6. Determination of the mechanism of inhibition of the compound BO1 towards Abl wild type and the AblT315I mutant. Reactions and data analysis were performed as described in Section 5. Values are the means of three independent experiments. Error bars represent \pm S.D. (A) Variations of the K_{mapp} (circles) or V_{maxapp} (triangles) values of Src reaction with ATP as the variable substrate determined as shown in Figure 5, as a function of BO1 concentrations. (B) Variations of the K_{mapp} (circles) or V_{maxapp} (triangles) values of Src reaction with peptide as the variable substrate determined as shown in Figure 5, as a function of BO1 concentrations. (C) As in panel A, but with the Abl enzyme. (D) As in panel B, but with the Abl enzyme. (E) Variation of the K_{mapp}^{ATP} (circles) or K_{mapp}^{pep} (triangles) of the AblT315I enzyme, determined as shown in Figure 5, as a function of BO1 concentration. (F) Variation of the V_{maxapp}^{ATP} (circles) or V_{maxapp}^{pep} (triangles) of the AblT315I enzyme, determined as shown in Figure 5, as a function of BO1 concentration.

Table 3
Inhibition of Src and Abl by SI178 and BO1 with respect to the reaction substrates

Inhibitor	K_i , μM	Variable substrate	Type of inhibition	Effects on binding constants	Molecular target
<i>Src</i> ^a					
SI178	0.1 ± 0.01	ATP	Competitive	Increases K_s^{ATP} , K_s^{pep}	Free enzyme
BO1	0.55 ± 0.03	Peptide	Competitive		
		ATP	Competitive	Increases K_s^{ATP} , K_s^{pep}	Free enzyme
		Peptide	Competitive		
Inhibitor	K_i , (K_i') ^b μM	Variable substrate	Type of inhibition	Effects on binding constants	Molecular target
<i>Abl</i> ^a					
SI178	0.7 ± 0.1 (3 ± 0.5)	ATP	Mixed	Increases K_s^{ATP}	Free enzyme; [E:ATP] complex
	0.75 ± 0.05	Peptide	Competitive	Increases K_s^{pep}	
				Decreases V_{max}	
BO1	0.1 ± 0.01	ATP	Competitive	Increases K_s^{ATP}	Free enzyme; [E:pep] complex
	0.12 ± 0.01 (0.47 ± 0.1)	Peptide	Mixed	Increases K_s^{pep}	
				Decreases V_{max}	
Inhibitor	K_i , μM	Variable substrate	Type of inhibition	Effects on binding constants	Molecular target
<i>AblT315I</i> ^a					
BO1	0.4 ± 0.1	ATP	Non-competitive	Decreases V_{max}	All forms
	0.45 ± 0.1	Peptide	Non-competitive	Decreases V_{max}	All forms

^a Values are the means of three independent experiments ± S.D.

^b In the case of mixed-type inhibition. See Figure 6B.

2.6. The compounds BO1 (3) and SI178 (4) target different enzymatic forms in the Src versus Abl reaction pathways

The data summarized in Table 3 allowed to identify the affected reaction steps and the enzymatic forms targeted by these inhibitors along the reaction pathway (Fig. 2). The proposed mechanism of action of the inhibitors is summarized in Figure 7. In the case of Src, both compounds targeted the free enzyme (Fig. 7A). After the formation of the enzyme–inhibitor complex, neither ATP, nor the peptide were anymore able to bind to the enzyme. In the case of Abl, the situation is more complex (Fig. 7B). The inhibition mechanisms listed in Table 3 suggest that BO1 and SI178 target both the free enzyme and the enzyme–peptide complex, preventing ATP binding. As reported above, SI178 and BO1 caused an increase of the K_{mapp} values for the ATP and peptide substrates, respectively, as well as a decrease of the corresponding V_{maxapp} values, resulting in a mixed-type inhibition. According to the reaction scheme (Fig. 7B), this can be explained by the fact that both inhibitors bind with higher affinity to the free enzyme than to the enzyme–substrate complex ($K_i < K_i'$). The K_i and K_i' values were derived according to Eq. (7) for a mixed-type mechanism, by studying the V_{maxapp} and K_{mapp} variations as a function of the inhibitor concentration, according to Eqs. (8) and (9). The resulting values are listed in Table 3. As can be seen, BO1 showed lower K_i and K_i' values than SI178. Thus, the higher potency of BO1 towards Abl with respect to SI178 depended from its ability to target both the free enzyme and the enzyme–substrate complex with higher affinity than SI178.

2.7. The compound BO1 (3) overcomes the T315I resistance mutation by altering its equilibrium dissociation constants for the different enzyme–substrate complexes

The T315I mutation can induce high level (>100-fold) resistance towards the clinically approved Abl inhibitor Imatinib. Developing novel effective inhibitors against this mutant is therefore of great pharmacological interest. Since BO1 was a more potent inhibitor of Abl wt with respect to SI178, we analyzed its inhibitory mechanism toward the AblT315I mutant. Primary plots are shown in Figure 5E, F and analysis of the variations of the K_{mapp} and V_{maxapp} values for both substrates are shown in Figure 6E and F. As can be seen, no changes could be observed in the K_{mapp} values for either substrate (Fig. 6E), whereas the inhibitor decreased the V_{maxapp} of

the reaction in dependence of both substrates (Fig. 6F). The calculated K_i values as well as the corresponding inhibitory mechanism are listed in Table 3. The proposed reaction equilibria are schematically drawn in Figure 7C. Against the AblT315I mutant, the compound BO1 acted as a purely non-competitive inhibitor with respect to both the ATP and peptide substrates, indicating that it was theoretically able to target the enzyme at any point along the reaction pathway, irrespectively of the presence of bound substrates. Thus, the T315I mutation induced a dramatic change in the binding mechanism of the BO1 inhibitor, without significantly affecting its apparent affinity (K_i), which was decreased only four-fold with respect to the wild type enzyme.

3. Discussion

One major limitation in the effectiveness of Abl-targeted therapy of chronic myeloid leukemia is the development of resistance towards Imatinib by Abl mutants, notably the T315I variant.^{3,16,17} This mutant is not effectively targeted by any of the second-generation Imatinib derivatives, such as dasatinib, nilotinib, bosutinib and INNO-406.^{7,18} Mass spectrometry analysis has revealed that, contrary to other mutations such as Y253H and E255V, the T315I substitution induces conformational changes in the Abl structure, particularly in the active site region (aminoacids 287–302) and in the SH3 linker domain.¹⁹ In accordance with this and other observations,²⁰ our results show that the T315I mutation alters the relative affinity of the enzyme for its substrates with respect to the wild type Abl. In addition, we demonstrate, for the first time, that the apo-enzyme mutant form shows lower affinity for both ATP and the peptide, than the corresponding binary complexes. These data suggest that mutant-specific drugs mimicking the natural substrates should be better designed on the basis of the enzyme–substrate complex structure, rather than the unliganded form.

The concept of multitargeted anticancer therapy is based on the possibility to simultaneously inhibit different molecular targets with one compound, in order to maximize the antiproliferative effects and minimize the development of drug resistance. The clinically used Abl inhibitor, Imatinib, has been shown to target also the tyrosine kinases KIT and PDGFR α ⁴ allowing its use also against gastrointestinal tumors and not only in chronic myeloid leukemia patients. The availability of dual Abl and Src inhibitors will undoubtedly prove extremely useful in light of the wider range of tumors whose proliferation depends on the action of these two kinases.^{21,22}

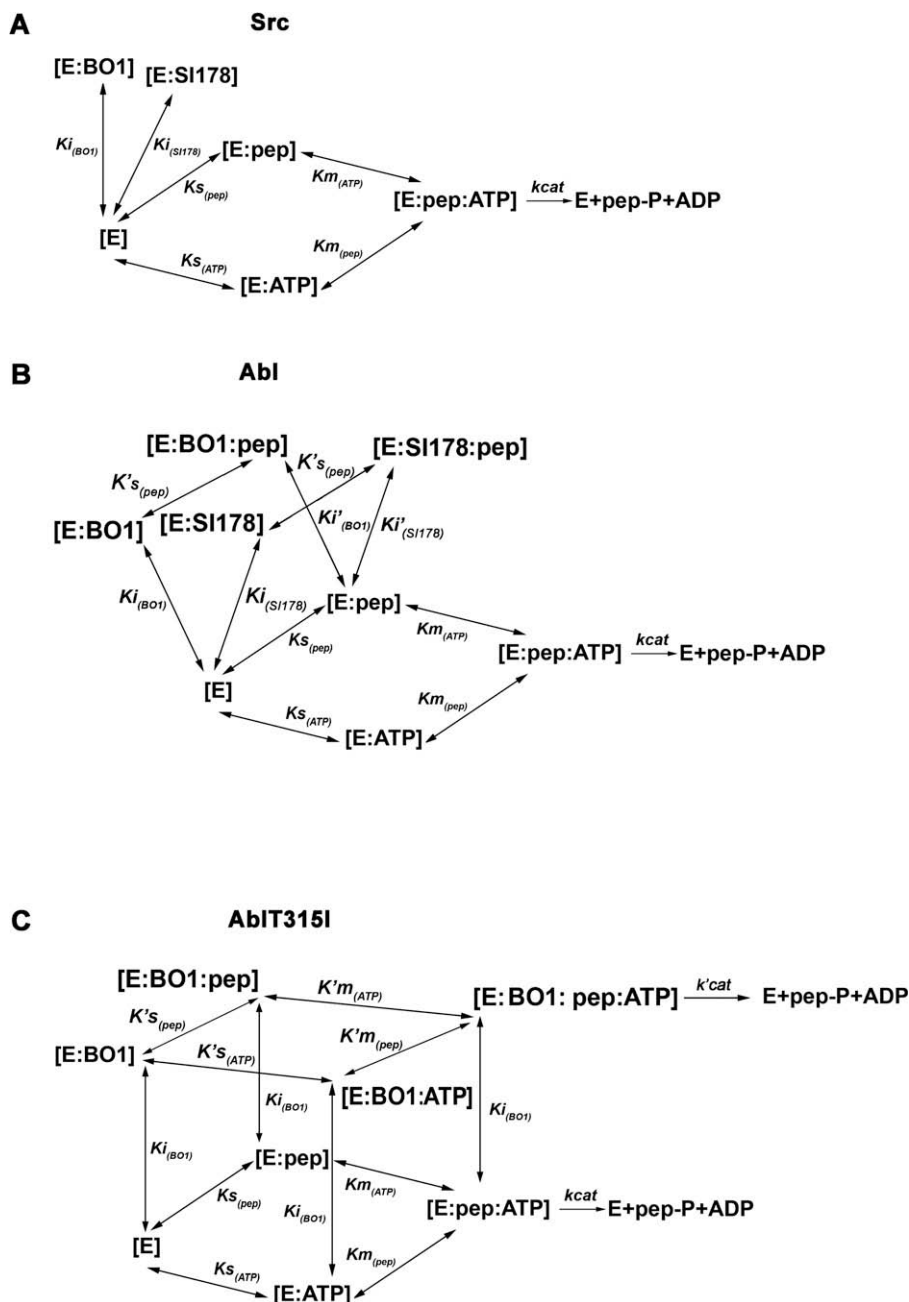


Figure 7. Different mechanisms of action of the compounds SI178 and BO1 towards Src and Abl. (A) Minimal reaction pathway for the inhibition of Src by SI178 and BO1. Both compounds act as competitive inhibitors with respect to both substrates (ATP, pep), being able to exclusively bind to the free enzyme with the apparent equilibrium dissociation constant K_i . (B) Minimal reaction pathway for the inhibition of wild type Abl by SI178 and BO1. Both compounds act as competitive inhibitors towards the ATP substrate only. This gives the possibility to two additional equilibrium binding steps: one with the free enzyme governed by the equilibrium dissociation constant K_i , and one with the binary complex of the enzyme and the peptide substrate [E:pep], governed by the equilibrium dissociation constant K'_i . Symmetrically, the peptide substrate can bind to either the free enzyme with an apparent equilibrium dissociation constant $K_{s(pep)}$ or to the enzyme–inhibitor complex, with apparent equilibrium dissociation constant $K'_{s(pep)}$. (C) Minimal reaction pathway for the inhibition of T315I Abl by BO1. The compound acts as non-competitive inhibitor with respect to both reactions substrates. Given the random mechanism of the reaction, the BO1 inhibitor can interact with each four enzymatic forms in the reaction pathway (here represented at the corners of the bottom square of a cubical three-dimensional space). Symmetrically, both substrates can interact with each enzyme–inhibitor complex (placed at the corners of the top square of the cube). This results in eight equilibrium binding steps. The assumption here is that the K_m and K_s values are equal to the corresponding K'_m and K'_s values. The catalytic rate K_{cat} is the rate of breakdown of the complex between enzyme and substrates ([E:BO1:pep:ATP]) to give the reaction products, whereas the K'_{cat} rate represents the breakdown of the complex between enzyme, inhibitor and substrates ([E:BO1:pep:ATP]). The model assumes that $K'_{cat} \ll K_{cat}$. For details see text.

Here we present a detailed enzymological characterization of the mechanism of action of two potent dual Src–Abl inhibitors. Our results clearly indicate that the selectivity of inhibition of the two enzymes depends on the particular form of the enzyme which is targeted by the inhibitor along the reaction pathway. In particular, Src inhibitors which are able to target also the Abl–peptide complex seem more potent than molecules targeting the Abl–ATP complex.

Finally, we show that the most potent derivative, BO1, can overcome the structural barrier imposed by the drug-resistant Abl mutant T315I by virtue of its ability to ‘adapt’ its mechanism of action to the specific enzymatic form of Abl: BO1 in fact was an ATP-competitive inhibitor of wild type Abl (targeting the free enzyme) while the same compound proved to act as a non-competitive inhibitor with respect to both the ATP and peptide substrates, in the case of Ab-

IT3151 (targeting all enzymatic forms). It is possible that BO1 acts as an allosteric inhibitor, not physically preventing ATP binding to the wild type enzyme, but rather inducing a very fast dissociation of the substrate from the enzyme–inhibitor complex, thus resulting in an apparent competitive mechanism. In agreement with this hypothesis, our kinetic data (Table 1) suggest that the structural rearrangement produced by the T3151 mutation allows a more stable binding of the ATP substrate to the enzyme–inhibitor complex. The resulting quaternary complex [E:BO1:pep:ATP], is either catalytically inactive or breaks down into products at a very reduced rate (Fig. 7C). The allosteric site responsible for the activity of BO1 on the AblT3151 mutant is still unknown and it is currently under investigation. Preliminary docking studies were performed with the known allosteric sites of Abl: (a) the binding site of myristate (PDB code: 1OPL); (b) the binding site of the recently reported T3151 inhibitor AP24534 (PDB code: 3IK3) which was shown to exploit both the ATP pocket and the deep allosteric pocket on the back of the gatekeeper residue. Unfortunately, docking and molecular dynamics simulation did not provide enough conclusive information to clearly draw a structure–activity relationship. Further experimental data are needed in order to clearly identify the allosteric pocket targeted by compound BO1. This is relevant, since most of dual Src–Abl inhibitors described to date are only moderately effective against this mutant^{6,23,24} and the identification of kinase inhibitors targeting sites other than the ATP cleft has emerged as a promising therapeutic option²⁵ as exemplified by the recent discovery of an allosteric Bcr–Abl inhibitor GNF-2.²⁶ It has to be noted that our BO1 compound described here shows only a modest loss of potency (fourfold) towards the AblT3151 mutant *in vitro* when compared to Imatinib (20-fold) or GNF-2 (40-fold), thus making it a very promising lead compound for the development of AblT3151 effective drugs.

4. Conclusion

Besides providing an explanation for the antiproliferative activity of BO1 against Imatinib-resistant leukemia cells, these data represent a detailed mechanistic background for the development of a novel class of dual Src–Abl inhibitors.

5. Experimental section

5.1. Chemicals

Labeled [γ -³²P]ATP was from GE Healthcare. All other chemical reagents were from Merck and Fluka.

5.2. Chemistry

The full synthesis and characterization of compound BO1 and related analogs have been already reported.^{8–10} The full synthesis and characterization of compound SI178 is reported in the [Supplementary data](#).

5.3. Enzymes and proteins

Baculovirus-produced recombinant purified his-tagged active human Src and Abl and the T3151 Abl mutant were purchased from Upstate (Lake Placid, NY).

5.4. Enzymatic assays

Src activity was measured in a filter-binding assay using a commercial kit (Src Assay Kit, Upstate), according to the manufacturer's protocol, using the specific Src peptide substrate [KVEKIGEGTYGV-

YYK] and in the presence of 0.125 pmol of Src and 0.160 pmol of [γ -³²P]ATP. Unlabeled ATP was added to reach the final concentrations as indicated in the figure legends. Abl activity was measured in a filter-binding assay using an Abl specific peptide substrate (Abtide, Upstate). Reaction conditions were (in a final volume of 10 μ l): 25 mM Tris–HCl pH 7.5, 1 mM DTT, 0.012 μ M [γ -³²P]ATP, 0.022 μ M c-Abl. Unlabeled ATP/Mg⁺⁺ (1:1 M/M) mix was added to reach the final ATP concentrations as indicated in the figure legends. Reactions were incubated 10 min at 30 °C. The samples (9 μ l) were spotted on paper cellulose filters which were washed according to the manufacturer's protocol. Filter-bound radioactivity was measured by liquid scintillation with a Microbeta-Trilux apparatus (Perkin–Elmer).

5.5. Kinetic analysis

The kinetic model for a sequential bi–bi (two substrates–two products) reaction mechanism, as depicted in Figure 2, is described by the equation:

$$v = V_{\max}/(1 + (K_m^{\text{ATP}}/[ATP]) + (K_m^{\text{pep}}/[pep]) + (K_s^{\text{ATP}} \cdot K_m^{\text{pep}}/[ATP] \cdot [pep])) \quad (1)$$

where [ATP] and [pep] are the concentrations of the ATP and peptide substrates, respectively, V_{\max} is the apparent maximal rate of the reaction and K_m and K_s for both substrates are as defined in Figure 2.

The K_s^{ATP} and K_s^{pep} were derived from the equations:

$$K_{\text{mapp}}[\text{pep}] = K_m^{\text{pep}}/(1 + [ATP]/K_s^{\text{ATP}}) \quad (2)$$

$$K_{\text{mapp}}[\text{ATP}] = K_m^{\text{ATP}}/(1 + [pep]/K_s^{\text{pep}}) \quad (3)$$

$$K_{\text{mapp}}[\text{pep}] = K_m^{\text{pep}} \cdot (1 + [ATP]/K_s^{\text{ATP}}) \quad (4)$$

$$K_{\text{mapp}}[\text{ATP}] = K_m^{\text{ATP}} \cdot (1 + [pep]/K_s^{\text{pep}}) \quad (5)$$

where K_{mapp} are the apparent Michaelis constant (K_m) values for one substrate obtained in the presence of varying concentrations of the other substrate.

The experimentally calculated values were applied to the relationship:

$$K_s^{\text{ATP}} \cdot K_m^{\text{pep}} = K_m^{\text{ATP}} \cdot K_s^{\text{pep}} \quad (6)$$

The mixed-type inhibition mechanism observed with Abl, was analyzed according to the equation:

$$v = V_{\max}/((K_s/[S]) \cdot (1 + [I]/K_i) + (1 + [I]/K'_i)) \quad (7)$$

where K_i is the apparent dissociation constant of the inhibitor for the free enzyme and K'_i is the apparent dissociation constant of the inhibitor for the enzyme–substrate complex.

Inhibitory constants for the fully non-competitive (K_i) mechanism observed with AblT3151 and the mixed-type (non-competitive term K'_i) mechanism observed with Abl, were calculated from the relationship:

$$K_i = [I]/((V_{\max}/V_{\text{maxapp}}) - 1) \quad (8)$$

where V_{maxapp} are the apparent maximal reaction rates measured in the presence of the inhibitor.

The inhibitory constant (K_i) for the competitive mechanism (observed with Src) and mixed-type (competitive term K_i) mechanism observed with Abl were calculated from the relationship:

$$K_i = [I]/((K_{\text{mapp}}/K_m) - 1) \quad (9)$$

where K_{mapp} are the apparent Michaelis constants (K_m) for the competing substrate measured in the presence of the inhibitor.

Curves were obtained by non-linear least squares computer fitting of the data to the equations above with the program GraphPad Prism 3.0.

Acknowledgements

Work in authors' laboratories was partially supported by an AIRC-Investigator Grant 2008 and a National Interest Research Project Grant PRIN_2007_N7KYCY to G.M. E.C. is the recipient of a FIRC Fellowship 2008–2010. S.Z. is the recipient of a Fondazione Buzzati-Traverso Fellowship.

Supplementary data

Supplementary data (experimental procedures and compound characterization) associated with this article can be found, in the online version, at doi:10.1016/j.bmc.2010.04.024.

References and notes

- Warmuth, M.; Damoiseaux, R.; Liu, Y.; Fabbro, D.; Gray, N. *Curr. Pharm. Des.* **2003**, *9*, 2043.
- Grunwald, V.; Soltan, J.; Ivanyi, P.; Rentschler, J.; Reuter, C.; Drevs, J. *Onkologie* **2009**, *32*, 129.
- Piccaluga, P. P.; Paolini, S.; Martinelli, G. *Cancer* **2007**, *110*, 1178.
- Druker, B. J. *Adv. Cancer Res.* **2004**, *91*, 1.
- Konig, H.; Copland, M.; Chu, S.; Jove, R.; Holyoake, T. L.; Bhatia, R. *Cancer Res.* **2008**, *68*, 9624.
- Schenone, S.; Manetti, F.; Botta, M. *Mini Rev. Med. Chem.* **2007**, *7*, 191.
- Noronha, G.; Cao, J.; Chow, C. P.; Dneprovskaia, E.; Fine, R. M.; Hood, J.; Kang, X.; Klebansky, B.; Lohse, D.; Mak, C. C.; McPherson, A.; Palanki, M. S.; Pathak, V. P.; Renick, J.; Soll, R.; Zeng, B. *Curr. Top. Med. Chem.* **2008**, *8*, 905.
- Carraro, F.; Pucci, A.; Naldini, A.; Schenone, S.; Bruno, O.; Ranise, A.; Bondavalli, F.; Brullo, C.; Fossa, P.; Menozzi, G.; Mosti, L.; Manetti, F.; Botta, M. *J. Med. Chem.* **2004**, *47*, 1595.
- Carraro, F.; Naldini, A.; Pucci, A.; Locatelli, G. A.; Maga, G.; Schenone, S.; Bruno, O.; Ranise, A.; Bondavalli, F.; Brullo, C.; Fossa, P.; Menozzi, G.; Mosti, L.; Modugno, M.; Tintori, C.; Manetti, F.; Botta, M. *J. Med. Chem.* **2006**, *49*, 1549.
- Manetti, F.; Pucci, A.; Magnani, M.; Locatelli, G. A.; Brullo, C.; Naldini, A.; Schenone, S.; Maga, G.; Carraro, F.; Botta, M. *ChemMedChem* **2007**, *2*, 343.
- Santucci, M. A.; Corradi, V.; Mancini, M.; Manetti, F.; Radi, M.; Schenone, S.; Botta, M. *ChemMedChem* **2009**, *4*, 118.
- Manetti, F.; Locatelli, G. A.; Maga, G.; Schenone, S.; Modugno, M.; Forli, S.; Corelli, F.; Botta, M. *J. Med. Chem.* **2006**, *49*, 327.
- Radi, M.; Crespan, E.; Botta, G.; Falchi, F.; Maga, G.; Manetti, F.; Corradi, V.; Mancini, M.; Santucci, M. A.; Schenone, S.; Botta, M. *Bioorg. Med. Chem. Lett.* **2008**, *18*, 1207.
- Manetti, F.; Falchi, F.; Crespan, E.; Schenone, S.; Maga, G.; Botta, M. *Bioorg. Med. Chem. Lett.* **2008**, *18*, 4328.
- Falchi, F.; Manetti, F.; Carraro, F.; Naldini, A.; Maga, G.; Crespan, E.; Schenone, S.; Bruno, O.; Brullo, C.; Botta, M. *ChemMedChem* **2009**, *4*, 976.
- Gora-Tybor, J.; Robak, T. *Curr. Med. Chem.* **2008**, *15*, 3036.
- Schenone, S.; Bruno, O.; Radi, M.; Botta, M. *Med. Res. Rev.* **2009** doi:10.1002/med.20175, in press.
- Tanaka, R.; Kimura, S. *Expert Rev. Anticancer Ther.* **2008**, *8*, 1387.
- Iacob, R. E.; Pene-Dumitrescu, T.; Zhang, J.; Gray, N. S.; Smithgall, T. E.; Engen, J. R. *Proc. Natl. Acad. Sci. U.S.A.* **2009**, *106*, 1386.
- Griswold, I. J.; MacPartlin, M.; Bumm, T.; Goss, V. L.; O'Hare, T.; Lee, K. A.; Corbin, A. S.; Stoffregen, E. P.; Smith, C.; Johnson, K.; Moseson, E. M.; Wood, L. J.; Polakiewicz, R. D.; Druker, B. J.; Deininger, M. W. *Mol. Cell. Biol.* **2006**, *26*, 6082.
- Rucci, N.; Susa, M.; Teti, A. *Anticancer Agents Med. Chem.* **2008**, *8*, 342.
- Li, S. *Leuk. Lymphoma* **2008**, *49*, 19.
- Martinelli, G.; Soverini, S.; Rosti, G.; Baccarani, M. *Leukemia* **2005**, *19*, 1872.
- Quintas-Cardama, A.; Kantarjian, H.; Cortes, J. *Future Oncol.* **2006**, *2*, 655.
- Bogoyevitch, M. A.; Fairlie, D. P. *Drug Discovery Today* **2007**, *12*, 622.
- Zhang, J.; Adrián, F. J.; Jahnke, W.; Cowan-Jacob, S. W.; Li, A. G.; Iacob, R. E.; Sim, T.; Powers, J.; Dierks, C.; Sun, F.; Guo, G. R.; Ding, Q.; Okram, B.; Choi, Y.; Wojciechowski, A.; Deng, X.; Liu, G.; Fendrich, G.; Strauss, A.; Vajpai, N.; Grzesiek, S.; Tuntland, T.; Liu, Y.; Bursulaya, B.; Azam, M.; Manley, P. W.; Engen, J. R.; Daley, G. Q.; Warmuth, M.; Gray, N. S. *Nature* **2010**, *463*, 501.